

Structure and Function of a Nitrifying Biofilm as Determined by In Situ Hybridization and the Use of Microelectrodes

ANDREAS SCHRAMM,¹ LARS HAUER LARSEN,² NIELS PETER REVSBECH,²
NIELS BIRGER RAMSING,² RUDOLF AMANN,^{1*}
AND KARL-HEINZ SCHLEIFER¹

*Technische Universität München, Lehrstuhl für Mikrobiologie, D-80290 Munich, Germany,¹
and Department of Microbial Ecology, Institute of Biological Sciences,
University of Aarhus, DK-8000 Aarhus C, Denmark*

Received 5 March 1996/Accepted 9 August 1996

Microprofiles of O₂ and NO₃⁻ were measured in nitrifying biofilms from the trickling filter of an aquaculture water recirculation system. By use of a newly developed biosensor for NO₃⁻, it was possible to avoid conventional interference from other ions. Nitrification was restricted to a narrow zone of 50 μm on the very top of the film. In the same biofilms, the vertical distributions of members of the lithoautotrophic ammonia-oxidizing genus *Nitrosomonas* and of the nitrite-oxidizing genus *Nitrobacter* were investigated by applying fluorescence in situ hybridization of whole fixed cells with 16S rRNA-targeted oligonucleotide probes in combination with confocal laser-scanning microscopy. Ammonia oxidizers formed a dense layer of cell clusters in the upper part of the biofilm, whereas the nitrite oxidizers showed less-dense aggregates in close vicinity to the *Nitrosomonas* clusters. Both species were not restricted to the oxic zone of the biofilm but were also detected in substantially lower numbers in the anoxic layers and even occasionally at the bottom of the biofilm.

Lithoautotrophic nitrification is a two-step process in which the combined action of ammonia- and nitrite-oxidizing bacteria results in the transformation of NH₃ to NO₃⁻ via NO₂⁻. It can lead to significant loss of fertilizer nitrogen in soil and to nitrate pollution of groundwater and surface water (40). On the other hand, nitrification is the initial step of total nitrogen removal from sewage via denitrification. There, it is important to prevent eutrophication of receiving waters or at least—when denitrification fails—to avoid contamination of receiving waters with ammonium salts that are toxic to most fish species (38).

Increased attention has, therefore, been paid to the physiology and ecology of nitrifying bacteria during the last decade. The genera *Nitrosomonas* and *Nitrobacter* are still the two best-known catalysts of the two respective steps (7, 29), but recent studies of nitrification have resulted in the isolation of new species (e.g., see references 8 and 28), and the discovery of unexpected metabolic steps (for example, see references 9 and 39). Various techniques for the determination of nitrification rates, e.g., by using nitrification inhibitors (23), ¹⁵N dilution techniques (27), or isotope pairing (46), have been developed. However, determination of the exact localization of nitrification and nitrifying bacteria remained difficult. Both the ammonia and the nitrite oxidizers are typical examples of fastidious bacteria. They are slowly growing bacteria and are difficult to enumerate by cultivation-dependent methods (5). Therefore, in situ identification methods have been evaluated. First, fluorescent-antibody techniques were used to detect and count nitrifiers microscopically (1, 6). However, because of the large serological diversity of ammonia oxidizers (6) and nonspecific bindings of fluorescent antibody to extracellular polymeric substances (48), these methods were not completely satisfying. More recently, progress in molecular ecology has enabled the

successful application of fluorescence in situ hybridization with 16S rRNA-targeted oligonucleotide probes in more complex environments as well (for a review, see reference 4). With this background, Wagner et al. could design a probe specific for halotolerant and halophilic members of the genus *Nitrosomonas* and successfully apply it to the detection of ammonia-oxidizing bacteria in activated sludge (51). Furthermore, two probes specific for all hitherto-sequenced species of *Nitrobacter* have been developed (52).

This introduction of a new, very powerful technique for in situ analysis of complex community structure coincided with the introduction of microelectrodes into the field of microbial ecology. These sensors make it possible today to monitor several metabolic reactions on a scale relevant for the study of stratified bacterial communities (for reviews, see references 43 and 45). For monitoring the nitrogen cycle, microsensors for nitrous oxide-oxygen (44), ammonia (15), and nitrate (14) have been developed and used for investigations in different habitats (12, 17, 24, 25, 36, 44). Despite an interference especially of HCO₃⁻ on the applied NO₃⁻ sensor, the work of Jensen et al. (24, 25) provides valuable information on the stratification of nitrifying activity and regulating effects of oxygen and ammonia. With a recently developed biosensor for nitrate (13, 31), it is, however, now possible to avoid the restrictions imposed by interfering ions.

In this study, we combined for the first time microprofiles of nitrification activity and data on the microdistribution of nitrifying bacteria in a biofilm. Fluorescent-oligonucleotide probing has already been applied to biofilm studies several times (e.g., see references 2 and 35). In a study of sulfate-reducing bacteria (SRB) in a trickling-filter biofilm, Ramsing et al. (41) had used this technique to relate the distribution of SRB to microprofiles of oxygen, sulfide, and pH. The present study was done with another trickling-filter biofilm treating the wastewater of an eel aquaculture. Growth of nitrifying bacteria was supported in this system by high concentrations of ammonia and stable temperatures of approximately 25°C. The relation between chemical gradients and the bacterial stratification is

* Corresponding author. Mailing address: Lehrstuhl für Mikrobiologie, Technische Universität München, Arcisstr. 16, D-80290 Munich, Germany. Phone: +49 89 2892 2373. Fax: +49 89 2892 2360. Electronic mail address: amann@mbitum2.biol.chemie.tu-muenchen.de.

TABLE 1. Probe sequences, target sites, and concentrations of formamide and NaCl in the hybridization or washing buffer, respectively, required for specific whole-cell in situ hybridization

Probe	Probe sequence	Target site (<i>Escherichia coli</i> rRNA positions)	% Formamide (hybridization buffer)	Concn of NaCl (washing buffer) (mM)
EUB338	5'-GCTGCCTCCCGTAGGAGT-3'	16S (338–355)	20	0.225
NEU23a	5'-CCCCTCTGCTGCACTCTA-3'	16S (653–670)	40	0.056
NIT2	5'-CGGGTTAGCGCACCGCT-3'	16S (1433–1450)	40	0.056
NIT3	5'-CCTGTGCTCCATGCTCCG-3	16S (1030–1047)	40	0.056
CNIT3	5'-CCTGTGCTCCAGGCTCCG-3	Used as competitor together with NIT3		
NON338	5'-ACTCCTACGGGAGGCAGC-3'	Nonbinding control	20	0.225

described, and possible reasons for the occurrence of nitrifiers in the anaerobic zone are discussed.

MATERIALS AND METHODS

Biofilm samples. The biofilms were grown on plastic foils, placed in a vertical position in the bottom part of a trickling filter. The filter was installed inside the water cycle of an aquaculture producing eels (Rostved, Denmark). The water which drenched the biofilm permanently contained various but high concentrations of NH_4^+ (0.3 to 7 mM) and NO_3^- (27 to 39 mM); the values for NO_2^- and N_2O were 0.7 to 11 μM and 0.2 to 0.9 μM , respectively. The whole plant was located in a closed dark room which made it possible to maintain a stable temperature between 20 and 28°C. After 3 to 4 months, the biofilm had reached a thickness of approximately 200 μm . All of the analyses were performed after the foil pieces had been removed and brought to the laboratory submerged in situ water.

Microelectrodes. Clark-type oxygen microelectrodes (42) with a 90% response time of less than 1 s and a negligible stirring sensitivity (<2%) were used to determine O_2 gradients at depth steps of 25 to 50 μm .

For measurements of NO_3^- profiles with a similar high resolution, a newly developed biosensor was used (13, 31). It was based on immobilized denitrifying bacteria (*Agrobacterium* sp.) which convert NO_3^- not to N_2 but only to N_2O . By placing the bacteria in a capillary in front of an electrochemical N_2O microsensor, the signal of the N_2O electrode was proportional to the concentration of NO_3^- . After optimization of its dimensions, the biosensor gave a linear response of from 0 to 300 μM NO_3^- , with 90% response times of approximately 20 s. The detection limit is approximately 3 μM NO_3^- . The only interfering substances were NO_2^- and N_2O , which were measured as NO_3^- and approximately $2 \times \text{NO}_3^-$, respectively. It was, therefore, necessary to check the production of NO_2^- and N_2O by chemical analysis and the use of a previously described combined microsensor for O_2 and N_2O (12).

Measuring setup. Immediately after sampling, the biofilm was transferred to a covered aquarium with air-bubbled in situ water kept at room temperature (22°C), and O_2 profiles were measured as described previously (e.g., see reference 45). A two-point calibration of the electrodes was made with 100% O_2 -saturated bulk water and the anoxic bottom of the film. The zero reading in the bottom of the biofilm was identical with the reading in N_2 -bubbled water. Then, we changed the in situ water to air-bubbled tap water, and NH_4^+ was added to a concentration of 300 μM . We assumed that a new steady-state situation was reached after 10 min. The water exchange was necessary because of the very high concentrations of N compounds in the eel farm water. A background of approximately 30 mM NO_3^- would have been too high for accurate determination of concentration changes in the micromolar range because of nitrifying activity in the biofilm.

The NO_3^- profiles were measured in the same way as that for O_2 , but a two-point calibration of the electrode in a corresponding aquatic medium containing no or 100 μM NO_3^- , respectively, was performed for every three or four profiles. To ensure equal temperature, the measuring setup served as a water bath for the calibration solutions.

Calibration of the N_2O sensor was done by adding certain amounts of N_2O -saturated water to the incubation water and using the values reported by Weiss and Price (53) for N_2O solubility.

Profiles of O_2 and NO_3^- were also recorded while the incubation water was only half-saturated with O_2 . The O_2 concentration was adjusted by flushing the water with a 1:1 mixture of atmospheric air and N_2 and was controlled with an O_2 sensor. The incubation time under reduced O_2 was approximately 4 h.

During all measurements, microelectrodes were mounted on a computer-controlled, motor-driven micromanipulator (Märtzhäuser Wetzlar GmbH, Wetzlar, Germany), and the entry of the electrode tip in the biofilm was monitored with a dissection microscope. Data acquisition was done automatically by a custom-built program on a personal computer.

Calculations. Oxygen uptake was determined from the O_2 profiles as the flux, J , through the diffusive boundary layer (DBL), whereas the total rate of nitrification was calculated from the NO_3^- profiles as the complete flux, J , away from the layer of NO_3^- production. Net fluxes were calculated by Fick's first law of diffusion (26): $J = (\delta C(x)/\delta x) \cdot D_s(x) \cdot \Phi(x)$, where $C(x)$ is the concentration of

the solute at the depth x , D_s is the apparent diffusion coefficient, and Φ is the porosity. We used table values of $2.24 \cdot 10^{-5} \text{ cm}^2 \text{ s}^{-1}$ (11) and $1.9 \cdot 10^{-5} \text{ cm}^2 \text{ s}^{-1}$ (32) for the diffusion coefficients of O_2 and NO_3^- , respectively, in water at 22°C. The diffusion coefficients in biofilms were assumed to be 40% lower than those in water, according to the measurements of $D_s \cdot \Phi$ performed by Revsbech et al. (44) and Glud et al. (22) with biofilms and microbial mats. Therefore, we used a value of $1.14 \cdot 10^{-5} \text{ cm}^2 \text{ s}^{-1}$ for $D_s \cdot \Phi$ of NO_3^- in the biofilm.

Chemical analysis. Water samples were taken from the trickling filter and from the measuring setup after the profiling to recalculate the $\text{NO}_3^-/\text{NO}_2^-$ ratio. The samples were stored at -20°C until photospectrometrical analysis for NH_4^+ , NO_2^- , and NO_3^- (10, 47, 49). For detection of N_2O , a Shimadzu GC-14A gas chromatograph equipped with an electron capture detector was used.

Biofilm fixation and cutting. Immediately after the microelectrode measurements, the biofilm samples were fixed in freshly prepared paraformaldehyde (4% in phosphate-buffered saline [PBS]) at 4°C for 1 h and were subsequently washed in PBS (3). Then, the biofilm side of the sample was embedded in OCT compound (Tissue-Tek II; Miles, Elkhart, Ind.) and placed above evaporating liquid N_2 (41). When frozen, the biofilm was removed from the plastic foil by slightly bending the substratum. Subsequently, the biofilm was embedded from its bottom and frozen again. To prevent the samples from thawing, the last steps were performed in the cryostat (Dittes-Duspiva, Heidelberg, Germany) at -20°C . In this instrument, 10- to 20- μm -thick vertical cryosections were cut. The sections were placed in five of the six hybridization wells on gelatin-coated microscopic slides and immobilized by air drying and dehydrating with 50, 80, and 96% ethanol (3). The slides were then stored at room temperature for as long as several weeks.

Reference cells. Different mixtures of known bacterial strains were deposited on the last well of the microscopic slides and served as internal controls for hybridization efficiency. Mixtures of the following species were used: *Nitrosomonas europaea* Nm57^T, *N. europaea* ATCC 25978^T/Nm50^T, and *Nitrobacter* sp. (donated by G. Rath, Institut für Botanik, Abteilung Mikrobiologie, Universität Hamburg [as positive controls]) and *Comamonas testosteroni* DSM 50244^T and *Bradyrhizobium japonicum* LMG 6138^T (donated by M. Wagner, Lehrstuhl für Mikrobiologie, Technische Universität München [as negative controls]).

Oligonucleotide probes. The following rRNA-targeted oligonucleotides (for sequences and target sites, see Table 1) were used: (i) EUB338, a general probe complementary to a region of the 16S rRNA of all bacteria as a positive control of hybridization efficiency (3); (ii) NEU23a, a probe specific for a region of the 16S rRNA of some lithoautotrophic ammonia-oxidizing bacteria (including *N. europaea* and *N. europaea*) as described recently by Wagner et al. (51); (iii) NIT2 and NIT3, probes specific for regions of the 16S rRNA of all hitherto-sequenced *Nitrobacter* strains (52); (iv) CNIT3, an unlabelled competitor to ensure the specificity of probe NIT3 when applied simultaneously (52); and (v) a negative-control probe, NON338, which is complementary to the probe EUB338 and, therefore, should be incapable of hybridization with rRNA of bacteria (34). The oligonucleotides were synthesized, labelled with the fluorescent dyes 5(6)-carboxy-fluorescein-*N*-hydroxysuccinimide ester (FLUOS; Boehringer Mannheim, Mannheim, Germany) and 5(6)-carboxy-tetramethylrhodamine succinimidyl-ester (CT; Molecular Probes Inc., Eugene, Ore.), and the hydrophilic sulphoindocyanine dye CY3 (monofunctional CY3.29-OSu; Biological Detection Systems, Pittsburgh, Pa.), and purified as described previously (3, 51).

In situ hybridization. For whole-cell hybridization of biofilm sections, the protocol described by Manz et al. (34) was used. Formamide was added to the final concentrations listed in Table 1 to ensure optimal hybridization stringency. All hybridizations were performed at a temperature of 46°C and an incubation time of 3 h. A stringent washing step was performed at 48°C for 10 min in a buffer containing 20 mM Tris-HCl (pH 8.0), 0.01% sodium dodecyl sulfate, and NaCl at the concentrations listed in Table 1.

Microscopy. Biofilm sections were examined with an Axioplan epifluorescence microscope (Carl Zeiss, Oberkochen, Germany) with Zeiss filter sets 09 and 15 and filter set CY3-HQ (Chroma Technology Corp., Brattleboro, Vt.). Color micrographs were taken on Kodak Ektachrome P1600 color reversal film. Exposure times were 0.01 s for phase-contrast micrographs and 10 to 20 s for epifluorescence micrographs. A Zeiss LSM 410 confocal laser-scanning microscope (Carl Zeiss), equipped with an Ar-ion laser (488 nm) and a HeNe laser (543 nm), was used to record optical sections as described by Wagner et al. (50).

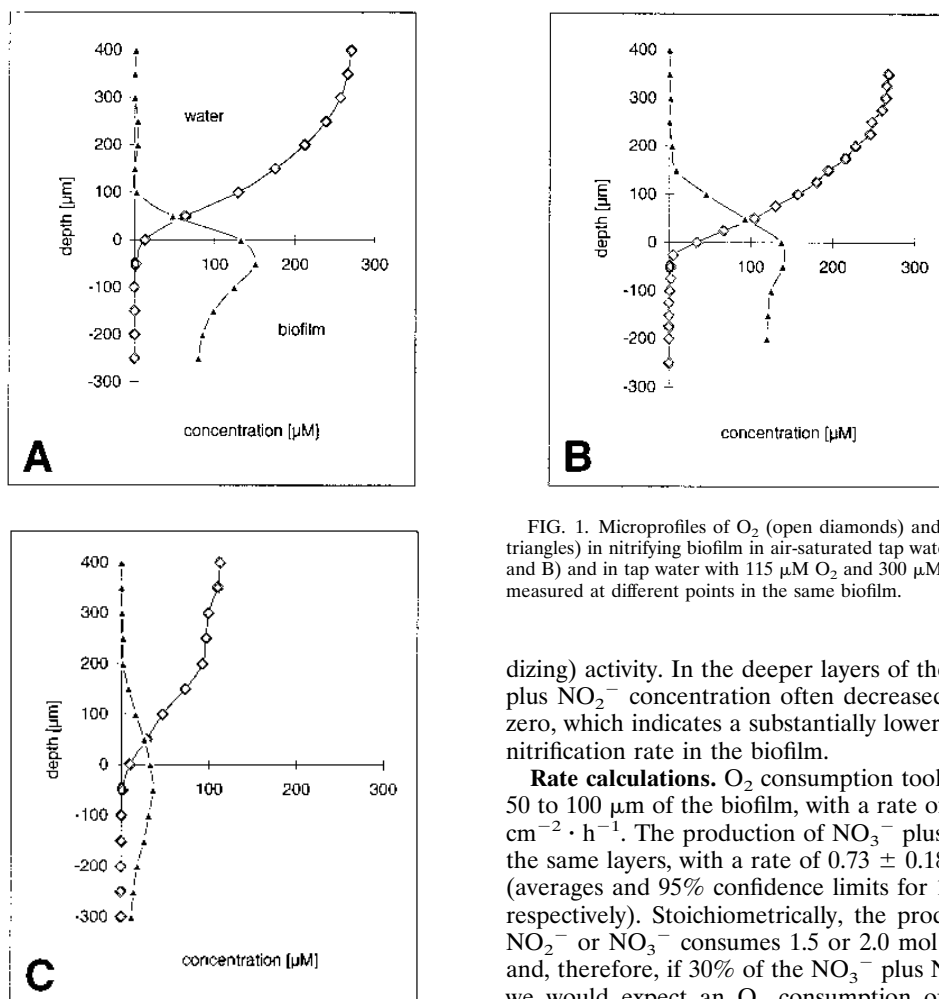


FIG. 1. Microprofiles of O_2 (open diamonds) and NO_3^- plus NO_2^- (filled triangles) in nitrifying biofilm in air-saturated tap water with $300 \mu M NH_4^+$ (A and B) and in tap water with $115 \mu M O_2$ and $300 \mu M NH_4^+$ (C). Profiles were measured at different points in the same biofilm.

Image processing, depth profiles, and three-dimensional reconstructions were performed with the standard software delivered with the instrument.

RESULTS

Microgradients. All O_2 profiles measured with fully O_2 -saturated water showed a decrease of O_2 within the DBL from $270 \mu M$ in the bulk water down to 20 to $60 \mu M$ on the biofilm surface. The thickness of the DBL varied between 150 and $250 \mu m$ because of a heterogeneous biofilm structure with protruding fluffy arms. O_2 penetrated approximately $100 \mu m$ into the biofilm, with fluctuations from 50 to $150 \mu m$. Two representative depth profiles are shown in Fig. 1A and B.

To interpret the NO_3^- microprofiles, it should be kept in mind that both NO_2^- and N_2O are also detected by the biosensor. Therefore, NO_2^- was determined chemically together with NO_3^- from the bulk water after incubation and profiling. NO_2^- amounted to as much as 30% of the NO_3^- values. Because of this high percentage, the profiles should be considered as combined NO_3^- plus NO_2^- profiles. The measured N_2O profiles display a slight increase of N_2O from zero in the bulk water up to a maximum concentration of $4 \mu M$ at approximately 150 to $200 \mu m$. The effect of N_2O was subtracted from the measured profiles, and the resulting combined NO_3^- plus NO_2^- profiles (Fig. 1) show a distinct peak just below the surface, indicating a high nitrifying (or at least ammonia-oxi-

dizing) activity. In the deeper layers of the biofilm, the NO_3^- plus NO_2^- concentration often decreased but never reached zero, which indicates a substantially lower denitrification than nitrification rate in the biofilm.

Rate calculations. O_2 consumption took place in the upper 50 to $100 \mu m$ of the biofilm, with a rate of $0.81 \pm 0.13 \mu mol \cdot cm^{-2} \cdot h^{-1}$. The production of NO_3^- plus NO_2^- appeared in the same layers, with a rate of $0.73 \pm 0.18 \mu mol \cdot cm^{-2} \cdot h^{-1}$ (averages and 95% confidence limits for 10 different profiles, respectively). Stoichiometrically, the production of 1 mol of NO_2^- or NO_3^- consumes 1.5 or 2.0 mol of O_2 , respectively, and, therefore, if 30% of the NO_3^- plus NO_2^- pool is NO_2^- , we would expect an O_2 consumption of approximately $1.2 \mu mol \cdot cm^{-2} \cdot h^{-1}$ only for nitrification. The discrepancy between the calculated O_2 demand for nitrification and the O_2 flux calculated from the O_2 profile will be discussed later. Denitrification in the layers below $150 \mu m$ ranged from 0 to $0.28 \mu mol \cdot cm^{-2} \cdot h^{-1}$, with an average of $0.11 \mu mol \cdot cm^{-2} \cdot h^{-1}$.

In situ water measurements. To check whether we changed the metabolism within the biofilm dramatically by substituting organic matter-containing in situ water with tap water plus nitrogen salts, we measured O_2 profiles before and after the substitution (data not shown). The depth penetration of O_2 did not change much, but a steeper concentration gradient in the DBL under in situ water (0.839 to $1.491 \mu mol \cdot cm^{-2} \cdot h^{-1}$, with an average of $1.216 \mu mol \cdot cm^{-2} \cdot h^{-1}$, compared with an average of $0.812 \mu mol \cdot cm^{-2} \cdot h^{-1}$ under enriched tap water) indicated a decrease in heterotrophic activity. A shift in oxygen uptake by 30% would usually result in a substantial change in oxygen penetration, but the penetration in the applied biofilm was so shallow that the change was masked by temporal and spatial heterogeneity.

In situ detection of nitrifiers. An extremely dense layer of ammonia oxidizers could be detected with probe NEU23a throughout the aerobic part, and a few clusters were also found in deeper parts of the biofilm. They formed characteristic aggregates as described for *Nitrosomonas* species (33) and as seen before in other habitats (51, 52) (Fig. 2B). In addition, *Nitrobacter* sp. was detected in the biofilm. Reliable visualization required the simultaneous use of both probes NIT2 and

NIT3. The colonies were less dense than the *Nitrosomonas* clusters and occurred in lower numbers than the dominating ammonia oxidizers. The maximum of this nitrite-oxidizing population was in the aerobic nitrification zone, but some single cells and colonies still existed in the upper anoxic layers (at a depth of 100 to 200 μm) and even occasionally on the bottom of the film (Fig. 2D). In general, *Nitrobacter* colonies and cells were more evenly distributed than the ammonia oxidizers.

In the oxic zone, investigation by confocal laser-scanning microscopy (CLSM) revealed a close coexistence of ammonia and nitrite oxidizers, supporting a sequential metabolism from ammonia to nitrate (Fig. 2E).

Oxygen effect. Incubation with reduced O_2 concentration (115 μM) decreased both O_2 penetration and metabolic rates. The O_2 concentration reached levels of less than 20 μM on the biofilm surface and zero within 25 to 75 μm of depth. The total oxygen uptake was $0.35 \pm 0.07 \mu\text{mol} \cdot \text{cm}^{-2} \cdot \text{h}^{-1}$, whereas the production of NO_3^- plus NO_2^- decreased to $0.28 \pm 0.14 \mu\text{mol} \cdot \text{cm}^{-2} \cdot \text{h}^{-1}$ (averages and 95% confidence limits for 10 different profiles, respectively). The main activity of nitrification was found at a depth of approximately 20 to 50 μm , and denitrification occurred in the deeper layers (100 to 200 μm), with an average rate of $0.10 \mu\text{mol} \cdot \text{cm}^{-2} \cdot \text{h}^{-1}$. Again, the O_2 consumption was approximately 30% lower than that required for the measured nitrification rate (see Discussion). Representative profiles of O_2 and NO_3^- plus NO_2^- , respectively, are shown in Fig. 1C. As expected in a short-term experiment with slowly growing autotrophic nitrifiers, no change in their spatial distribution could be seen.

DISCUSSION

Microprofiles. It has long been difficult to obtain accurate microprofiles of nitrification. One of the problems of the LIX electrodes for NO_3^- used in the study described by Jensen et al. (24), was the interference of HCO_3^- (selectivity coefficient, 0.006) and, therefore, the need to perform measurements at artificial low alkalinities. However, the HCO_3^- production of biologically active biofilms and sediments does create steep concentration gradients within these systems. Thus, even with low concentrations of HCO_3^- in the overlying water, its biogenic accumulation resulted in inaccurate NO_3^- determination within the biofilm when the concentrations were less than approximately 25 μM (24). With the new biosensor, these problems were avoided, since the only agents interfering with the determination of NO_3^- are NO_2^- and N_2O . The additive determination of NO_3^- plus NO_2^- by the biosensor may be an advantage in some contexts. In the present investigation, it made it possible to determine the activity of NH_4^+ oxidation without having to consider how much of the intermediate NO_2^- was further oxidized to NO_3^- . For a detailed study of NO_2^- oxidation and the synergism between NH_4^+ and NO_2^- oxidizers, however, a microsensor for NO_2^- would be necessary. Such a microsensor was not available during this investigation.

The nitrifying activity of approximately $0.8 \mu\text{mol} \cdot \text{cm}^{-2} \cdot \text{h}^{-1}$ found in this study is very high compared with previous microsensor studies of nitrifying sediments (24) but is comparable to rates found at the surface of manure clumps in soil (37). The nitrifying layer in the investigated biofilm was only approximately 25 μm thick, indicating extremely high specific rates of approximately $30 \mu\text{mol} \cdot \text{cm}^{-3} \cdot \text{h}^{-1}$. The manure-soil interface was analyzed by ^{15}N isotope techniques, and we do not know the exact thickness of the nitrifying layer in this system, but diffusion-reaction models indicated that the zone was very narrow. Such narrow zones with extremely high nitrifi-

cation activities are possible only when both NH_4^+ and O_2 are supplied to the active layers in adequate amounts. For oxygen, this is possible only by diffusion from a thoroughly mixed phase of overlying water to a superficial nitrification zone in the case of the biofilm or by gas phase diffusion in the case of the manure-soil system. It is difficult to obtain highly active pure cultures of nitrifying bacteria; however, judging from our environmental data, this must be due to unsuitable culture conditions.

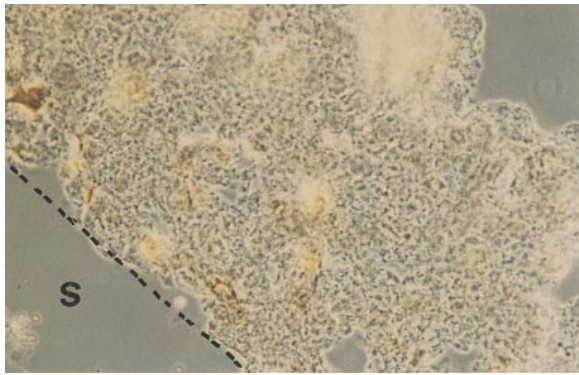
The oxygen flux as calculated from the oxygen profile was too small to account for the nitrifying activity. A likely explanation is a local change in water current imposed by the microsensor. It has been shown that even microsensors with tips of a few micrometers cause such changes and that the diffusive boundary layer is eroded down to smaller thickness when a microsensor tip is inserted (21). Larger tips will result in a more vigorous erosion than thin tips, and since the biosensor was approximately 30 μm thick, compared with the 10- μm -thick oxygen microsensor, this could account for the observed discrepancy. The effect can actually be seen in Fig. 1, where near-constant water phase concentrations of NO_3^- were reached at approximately 100 to 150 μm above the biofilm, whereas the distance for oxygen was 200 to 300 μm . In future studies, it would be advisable to use microsensors of similar physical dimensions near the tip so that the data correspond to the same hydraulic regime.

Denitrification was heterogeneously distributed, but the rates were generally low. The concentration of NO_3^- plus NO_2^- was high throughout the anoxic layers of the biofilm; thus, the low level of activity is very likely due to a shortage of suitable organic electron donors. This argument is strongly supported by measuring denitrification at low oxygen concentrations; despite an increased anoxic zone and sufficient NO_3^- plus NO_2^- supply, the rate of denitrification remained the same. However, there is no doubt that the denitrification activity measured in our experiments was lower than that occurring in situ. This is a direct consequence of the substitution of the in situ water with tap water containing additional inorganic N salt, such that denitrifiers could use only organic compounds produced in the biofilm.

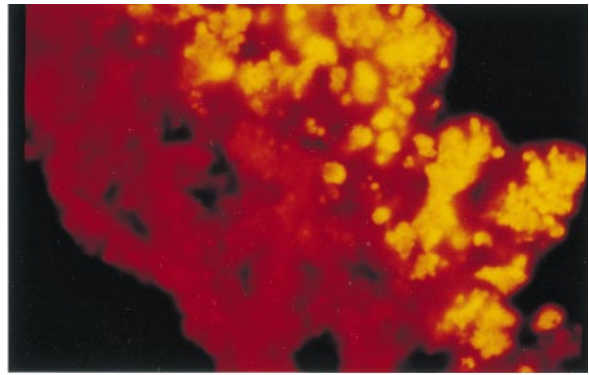
Stratification of nitrifiers. The dominance of chemolithoautotroph-nitrifying bacteria in the aerobic part of the biofilm is interesting, since they are considered to be poor competitors with heterotrophs (19). Reasons for a low level of competitiveness of the nitrifiers are high K_m values for oxygen compared with those for heterotrophs (16 μM for *Nitrosomonas* species and 62 μM for *Nitrobacter* species, but $<1 \mu\text{M}$ for most of the heterotrophs) and slow growth (5). Obviously, there was a limited supply of easily degradable organic matter, whereas NH_4^+ was close to the optimum concentration of 2 to 10 mM (7, 29). Furthermore, the moderate and constant temperatures of the eel farm trickling filter at approximately 25°C supported the nitrifying bacteria, which are known to be especially bad competitors at cold temperatures.

It is obvious that oxygen is the limiting factor for both nitrification activity and abundance of the nitrifying population, since oxygen penetration, high rates of nitrification, and high numbers of nitrifiers are well correlated in the upper 50 μm of the biofilm. Although oxygen was present down to 100 μm , its concentration reached the K_m values of nitrifiers and therefore became limiting. In contrast, no depletion of NH_4^+ is expected in situ at substrate concentrations of a few micromolar, and even in the experimental setup, saturation with NH_4^+ is most likely, but this should be confirmed in future studies by additional use of an NH_4^+ microsensor.

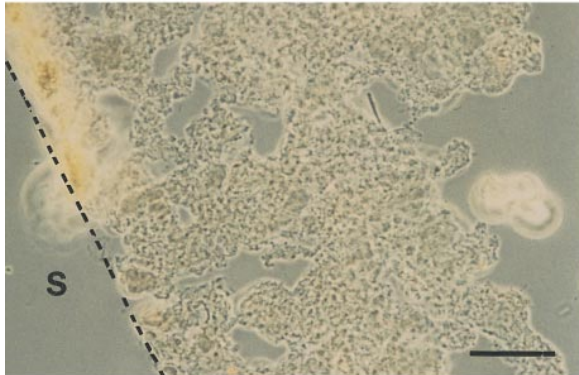
As previously reported from other anaerobic environments



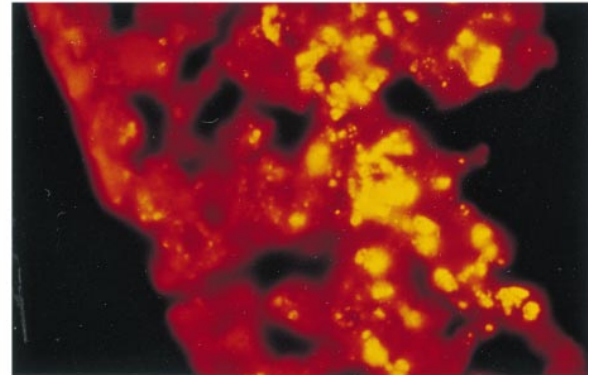
A



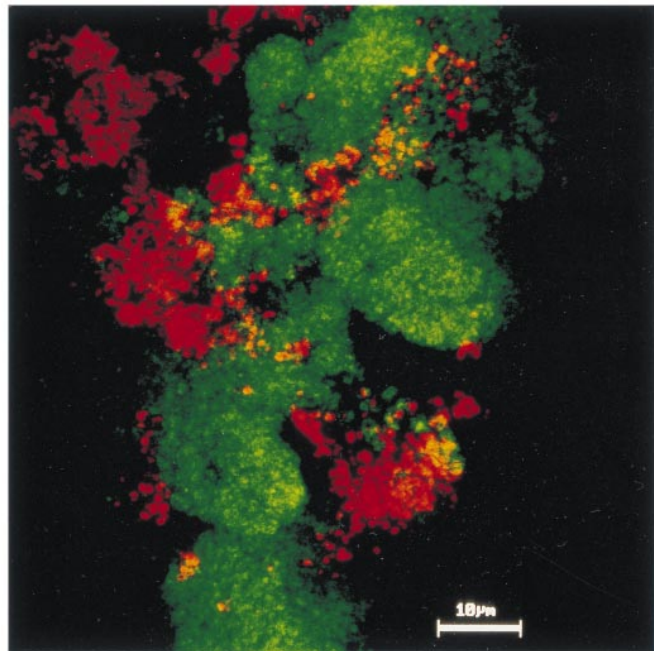
B



C



D



E

FIG. 2. In situ hybridizations of vertical biofilm sections. (A and B) Phase-contrast and epifluorescence micrographs, respectively, after hybridization with CY3-labelled probe NEU23a. (C and D) Phase-contrast and epifluorescence micrographs, respectively, after hybridization with a combination of CY3-labelled probes NIT2 and NIT3. With the CY3 HQ-filter set, probe-conferred CY3 fluorochromes are visualized in yellow, whereas autofluorescence of the biofilm appears in red (magnification, $\times 400$; scale bar, $50 \mu\text{m}$, S, substratum). (E) CLSM projection (all in focus) of a $20\text{-}\mu\text{m}$ -thick biofilm section after simultaneous hybridization with FLUOS-labelled probe NEU23a (green) and CT-labelled probes NIT2 and NIT3 (red). Only a detail of 78 by $78 \mu\text{m}$ from the nitrification zone is shown; the biofilm surface is on the right. Yellow signals do not yield from binding of both probes to one cell but are the result of overlaying red and green cells. Background fluorescence was reduced by the CLSM technique (magnification, $\times 1,000$; scale bar, $10 \mu\text{m}$).

(e.g., see reference 1), small numbers of nitrifiers were present in the deeper layers of the biofilm. There may be several explanations for the survival of nitrifiers in these layers. (i) Because of hydraulic flow within pores of the biofilm (16), oxic microniches may have existed in deeper layers. Such locally deep oxygen penetration was never detected during our microsensor work in the laboratory, but the hydraulic conditions in our setup could be very different from those in the trickling filter. (ii) Formerly oxic layers might have been overgrown during biofilm development. It has been shown that some bacteria, including *Nitrosomonas* species, are able to maintain their ribosome content during periods of nutrient starvation or inhibition (18, 51). (iii) Anaerobic metabolisms such as a combined ammonia oxidation-denitrification (9, 30) or dissimilatory reduction of NO_3^- with organic electron donors (20) may enable the survival of ammonia oxidizers and nitrite oxidizers, respectively, during periods without or at low concentrations of oxygen. For further investigation of the anaerobic *Nitrobacter* cells, a nitrite microsensor would be a useful tool to monitor specifically their metabolism in situ.

The close vicinity of ammonia and nitrite oxidizers as shown by the CLSM is a direct result of the sequential metabolism of ammonia via nitrite to nitrate. By this spatial arrangement, the diffusion path from the *Nitrosomonas* clusters to the surrounding *Nitrobacter* cells is extremely short and facilitates an efficient transfer of the intermediate NO_2^- . When considering the K_m values for oxygen of *Nitrosomonas* species and *Nitrobacter* species (see above), it is obvious that *Nitrosomonas* species could outcompete *Nitrobacter* species for oxygen under the low-oxygen concentrations obtained in the nitrification zone, and this could be one reason for the accumulation of nitrite in the bulk water. Additionally, dissimilatory reduction of nitrate to nitrite, nitric acid, or nitrous oxide, which is performed by *Nitrobacter* species in the anoxic layers (20), would be another source of nitrite in the system. The different K_m values for oxygen could also result in the different cluster size, since *Nitrosomonas* cells formed large ball-shaped clusters of as much as 50 μm , whereas the *Nitrobacter* colonies generally appear to be smaller and more irregular. Perhaps *Nitrobacter* cells are forced to disaggregate at a smaller size than *Nitrosomonas* cells because of oxygen depletion in the center of the cluster to levels less than their K_m values.

In conclusion, the combination of a microsensor technique with specific oligonucleotide probes provides reliable and direct information about nitrification as it occurs in nature. Data on community structure can be related to the metabolic functions of the respective populations. For further detailed investigations, microsensors for nitrite and additional oligonucleotide probes for nitrifiers are under development.

ACKNOWLEDGMENT

This work was supported by the Körber Preis to N.P.R., R.A., and K.H.S.

We thank Ole Krogh from Djurs Ål for cooperation in the aquaculture and Lars B. Pedersen (microelectrodes), Dorethe Jensen (cryostat), and Sibylle Schadhauer (oligonucleotides) for their excellent technical assistance. The help of P. Hutzler (GSF-Forschungszentrum für Umwelt und Gesundheit, Oberschleißheim, Germany), and A. Neef (Technical University Munich) in CLSM is acknowledged. For providing fixed cells and valuable comments on the manuscript, we gratefully appreciate G. Rath, H.-P. Koops (Hamburg), and M. Wagner (Munich).

REFERENCES

- Abeliovich, A. 1987. Nitrifying bacteria in wastewater reservoirs. *Appl. Environ. Microbiol.* **53**:754–760.
- Amann, R. I., J. Stromley, R. Devereux, R. Key, and D. A. Stahl. 1992.

- Molecular and microscopic identification of sulfate-reducing bacteria in multispecies biofilms. *Appl. Environ. Microbiol.* **58**:614–623.
- Amann, R. I., L. Krumholz, and D. A. Stahl. 1990. Fluorescent-oligonucleotide probing of whole cells for determinative, phylogenetic, and environmental studies in microbiology. *J. Bacteriol.* **172**:762–770.
- Amann, R. I., W. Ludwig, and K.-H. Schleifer. 1995. Phylogenetic identification and in situ detection of individual microbial cells without cultivation. *Microbiol. Rev.* **59**:143–169.
- Belser, I. W. 1979. Population ecology of nitrifying bacteria. *Annu. Rev. Microbiol.* **33**:309–333.
- Belser, I. W., and E. L. Schmidt. 1978. Serological diversity within a terrestrial ammonia-oxidizing population. *Appl. Environ. Microbiol.* **36**:589–593.
- Bock, E., and H.-P. Koops. 1992. The genus *Nitrobacter* and related genera, p. 2302–2309. In A. Balows, H. G. Trüper, M. Dworkin, W. Harder, and K.-H. Schleifer (ed.), *The prokaryotes*, 2nd ed. Springer-Verlag, New York.
- Bock, E., H.-P. Koops, U. C. Möller, and M. Rudert. 1990. A new facultatively nitrite oxidizing bacterium, *Nitrobacter vulgaris* sp. nov. *Arch. Microbiol.* **153**:105–110.
- Bock, E., I. Schmidt, R. Stüven, and D. Zart. 1995. Nitrogen loss caused by denitrifying *Nitrosomonas* cells using ammonium or hydrogen as electron donors and nitrite as electron acceptor. *Arch. Microbiol.* **163**:16–20.
- Bower, C. E., and T. Holm-Hansen. 1980. A salicylate-hypochlorite method for determining ammonia in seawater. *Can. J. Fish. Aquat. Sci.* **37**:794–798.
- Broecker, W. S., and T.-H. Peng. 1974. Gas exchange rates between air and sea. *Tellus* **26**:21–35.
- Dalsgaard, T., and N. P. Revsbech. 1992. Regulating factors of denitrification in trickling filter biofilms as measured with the oxygen/nitrous oxide microsensor. *FEMS Microbiol. Ecol.* **101**:151–164.
- Damgaard, L. R., L. H. Larsen, and N. P. Revsbech. 1995. Microscale biosensors for environmental monitoring. *Trends Anal. Chem.* **14**:300–303.
- DeBeer, D., and J.-P. R. A. Sweerts. 1989. Measurement of nitrate gradients with an ion-selective microelectrode. *Anal. Chim. Acta* **219**:351–356.
- DeBeer, D., and J. C. van den Heuvel. 1988. Response of ammonium-selective microelectrodes based on the neutral carrier nonactin. *Talanta* **35**:728–730.
- DeBeer, D., and P. Stoodley. 1995. Relation between the structure of an aerobic biofilm and transport phenomena. *Water Sci. Technol.* **32**:11–18.
- DeBeer, D., J. C. van den Heuvel, and S. P. P. Ottengraf. 1993. Microelectrode measurements of the activity distribution in nitrifying bacterial aggregates. *Appl. Environ. Microbiol.* **59**:573–579.
- Flårdh, K., P. S. Cohen, and S. Kjelleberg. 1992. Ribosomes exist in large excess over the apparent demand for protein synthesis during carbon starvation in marine *Vibrio* sp. Strain CCUG 15956. *J. Bacteriol.* **174**:6780–6788.
- Focht, D. D., and W. Verstraete. 1977. Biochemical ecology of nitrification and denitrification. *Adv. Microbiol. Ecol.* **1**:135–214.
- Freitag, A., M. Rudert, and E. Bock. 1987. Growth of *Nitrobacter* by dissimilatory nitrate reduction. *FEMS Microbiol. Lett.* **14**:105–109.
- Glud, R. N., J. K. Gundersen, N. P. Revsbech, and B. B. Jørgensen. 1994. Effects on the benthic diffusive boundary layer imposed by microelectrodes. *Limnol. Oceanogr.* **39**:462–467.
- Glud, R. N., K. Jensen, and N. P. Revsbech. 1995. Diffusivity in surficial sediments and benthic mats determined by use of a combined N_2O - O_2 microsensor. *Geochim. Cosmochim. Acta* **59**:231–237.
- Hall, G. H. 1984. Measurement of nitrification rates in lake sediments: comparison of the nitrification inhibitors nitrapyrin and allylthiourea. *Microb. Ecol.* **10**:25–36.
- Jensen, K., N. P. Revsbech, and L. P. Nielsen. 1993. Microscale distribution of nitrification activity in sediment determined with a shielded microsensor for nitrate. *Appl. Environ. Microbiol.* **59**:3287–3296.
- Jensen, K., N. P. Sloth, N. Risgaard-Petersen, S. Rysgaard, and N. P. Revsbech. 1994. Estimation of nitrification and denitrification from microprofiles of oxygen and nitrate in model sediment systems. *Appl. Environ. Microbiol.* **60**:2094–2100.
- Jørgensen, B. B., and N. P. Revsbech. 1985. Diffusive boundary layers and the oxygen uptake of sediment and detritus. *Limnol. Oceanogr.* **30**:11–21.
- Koike, I., and A. Hattori. 1977. Simultaneous determination of nitrification and nitrate reduction in coastal sediments by ^{15}N dilution technique. *Appl. Environ. Microbiol.* **35**:853–857.
- Koops, H.-P., B. Böttcher, U. C. Möller, A. Pommerening-Röser, and G. Stehr. 1991. Classification of eight new species of ammonia-oxidizing bacteria: *Nitrosomonas communis* sp. nov., *Nitrosomonas urea* sp. nov., *Nitrosomonas aestuarii* sp. nov., *Nitrosomonas marina* sp. nov., *Nitrosomonas nitrosa* sp. nov., *Nitrosomonas eutropha* sp. nov., *Nitrosomonas oligotropha* sp. nov., *Nitrosomonas halophila* sp. nov. *J. Gen. Microbiol.* **137**:1689–1699.
- Koops, H.-P., and U. C. Möller. 1992. The lithotrophic ammonia-oxidizing bacteria. p. 2625–2637. In A. Balows, H. G. Trüper, M. Dworkin, W. Harder, and K.-H. Schleifer (ed.), *The prokaryotes*, 2nd ed. Springer-Verlag, New York.
- Kuenen, J. G., and L. A. Robertson. 1994. Combined nitrification-denitrification processes. *FEMS Microbiol. Rev.* **15**:109–117.
- Larsen, L. H., N. P. Revsbech, and S. J. Binnerup. 1996. A microsensor for

- nitrate based on immobilized denitrifying bacteria. *Appl. Environ. Microbiol.* **62**:1248–1251.
32. **Li, Y.-H., and S. Gregory.** 1974. Diffusion of ions in sea water and in deep-sea sediments. *Geochim. Cosmochim. Acta* **38**:703–714.
 33. **Macdonald, R. M.** 1986. Nitrification in soil: an introductory history. *Spec. Publ. Soc. Gen. Microbiol.* **20**:1–16.
 34. **Manz, W., R. Amann, W. Ludwig, M. Wagner, and K.-H. Schleifer.** 1992. Phylogenetic oligodeoxynucleotide probes for the major subclasses of proteobacteria: problems and solutions. *Syst. Appl. Microbiol.* **15**:593–600.
 35. **Manz, W., U. Szewzyk, P. Eriksson, R. Amann, K.-H. Schleifer, and T. A. Stenström.** 1993. *In situ* identification of bacteria in drinking water and adjoining biofilms by hybridization with 16S and 23S rRNA-directed fluorescent oligonucleotide probes. *Appl. Environ. Microbiol.* **59**:2293–2298.
 36. **Nielsen, L. P., P. B. Christensen, N. P. Revsbech, and J. Sørensen.** 1990. Denitrification and oxygen respiration in biofilms studied with a microsensor for nitrous oxide and oxygen. *Microb. Ecol.* **19**:63–72.
 37. **Nielsen, T. H., and N. P. Revsbech.** 1994. Diffusion chamber for ¹⁵N determination of coupled nitrification-denitrification associated with organic hot-spots in soil. *Soil Sci. Soc. Am. J.* **58**:795–800.
 38. **Painter, H. A.** 1986. Nitrification in the treatment of sewage and wastewaters. *Spec. Publ. Soc. Gen. Microbiol.* **20**:185–213.
 39. **Poth, M.** 1986. Dinitrogen production from nitrite by a *Nitrosomonas* isolate. *Appl. Environ. Microbiol.* **52**:957–959.
 40. **Prosser, J. I. (ed.)** 1986. Nitrification. Society for General Microbiology, Oxford.
 41. **Ramsing, N. B., M. Köhl, and B. B. Jørgensen.** 1993. Distribution of sulfate-reducing bacteria, O₂, and H₂S in photosynthetic biofilms determined by oligonucleotide probes and microelectrodes. *Appl. Environ. Microbiol.* **59**:3840–3849.
 42. **Revsbech, N. P.** 1989. An oxygen microelectrode with a guard cathode. *Limnol. Oceanogr.* **34**:474–478.
 43. **Revsbech, N. P.** 1994. Analysis of microbial mats by use of electrochemical microsensors: recent advances, p. 149–163 *In* L. J. Stal and P. Caumette (ed.), *Microbial mats: structure, development, and environmental significance*. Springer, New York.
 44. **Revsbech, N. P., P. B. Christensen, L. P. Nielsen, and J. Sørensen.** 1989. Denitrification in a trickling filter biofilm studied by a microsensor for oxygen and nitrous oxide. *Water Res.* **23**:867–871.
 45. **Revsbech, N. P., and B. B. Jørgensen.** 1986. Microelectrodes: their use in microbial ecology. *Adv. Microb. Ecol.* **9**:293–352.
 46. **Rysgaard, S., N. Risgaard-Petersen, L. P. Nielsen, and N. P. Revsbech.** 1993. Nitrification and denitrification in lake and estuarine sediments measured by the ¹⁵N dilution technique and isotope pairing. *Appl. Environ. Microbiol.* **59**:2093–2098.
 47. **Strickland, J. D. H., and T. R. Parsons.** 1972. A practical handbook of seawater analysis. Bulletin 167. Fisheries Research Board of Canada, Ottawa.
 48. **Swierinski, H., S. Gaiser, and D. Bardtke.** 1985. Immunofluorescence for the quantitative determination of nitrifying bacteria: interference of the test in biofilm reactors. *Appl. Microbiol. Biotechnol.* **21**:125–128.
 49. **Velghe, N., and A. Claeys.** 1985. Rapid spectrophotometric determination of nitrate in mineral waters with resorcinol. *Analyst* **110**:313–314.
 50. **Wagner, M., B. Abmus, A. Hartmann, P. Hutzler, and R. Amann.** 1994. *In situ* analysis of microbial consortia in activated sludge using fluorescently labeled, rRNA-targeted oligonucleotide probes and confocal scanning laser microscopy. *J. Microscopy* **176**:181–187.
 51. **Wagner, M., G. Rath, R. Amann, H.-P. Koops, and K.-H. Schleifer.** 1995. *In situ* identification of ammonia-oxidizing bacteria. *Syst. Appl. Microbiol.* **18**:251–264.
 52. **Wagner, M., G. Rath, H.-P. Koops, J. Flood, and R. Amann.** 1996. *In situ* analysis of nitrifying bacteria in sewage treatment plants. *Water Sci. Tech.* **34**:237–244.
 53. **Weiss, R. F., and B. A. Price.** 1980. Nitrous oxide solubility in water and seawater. *Mar. Chem.* **8**:347–359.